Energy & Environmental Science

Accepted Manuscript

ROYAL SOCIETY OF CHEMISTRY

www.rsc.org/ees

Nanotechnology enabled rechargeable Li−SO_2 battery: Another approach towards post lithium-ion battery system

Goojin Jeong[a], Hansu Kim[b,*], Jong Hwan Park[a], Jaehwan Jeon[a,b], Xing Jin[c], Juhye Song[b], Bo-Ram Kim[b], Min-Sik Park[a], Ji Man Kim[c,*], Young-Jun Kim[a,*]

[a] Advanced Batteries Research Center, Korea Electronics Technology Institute, Seongnam, 463-816, Republic of Korea

[b] Department of Energy Engineering, Hanyang University, Seoul, 133-791, Republic of Korea

[c] Department of Chemistry, Sungkyunkwan University, Suwon, 440-746, Republic of Korea

* Corresponding author: khansu@hanayng.ac.kr,jimankim@skku.edu, yjkim@keti.re.kr

Abstract

Extensive research efforts have been devoted to the development of alternative battery chemistry to replace the current technology of lithium-ion batteries (LIBs). Here, we demonstrate that the Li−SO_2 battery chemistry, already established 30 years ago, has considerable potential to be regarded as a candidate for post-LIBs when proper nanotechnology is exploited. The recently developed nanostructured carbon materials greatly improve the battery performances of the Li−SO_2 cells, including a reversible capacity higher than 1000 mAh g^{-1} with a working potential of 3 V and excellent cycle performance over 150 cycles, and provide a theoretical energy density of about 651 Wh kg^{-1}, which is about 70% higher than that of the currently used LIB. The nanostructured carbon cathodes offer not only an enlarged active surface area, but also a mechanical buffer to accommodate insulating discharge products upon discharge. Considering the other outstanding properties of the SO_2-based inorganic electrolyte, such as non-flammability and significantly higher ionic conductivities, wisely selected nanotechnology renders the Li−SO_2 battery chemistry a very promising approach towards the development of a post-LIB system.

Keywords: Li−SO_2 rechargeable battery; post lithium-ion battery; nanostructured carbon; hierarchical meso-macropore; inorganic electrolyte

Introduction

Developing new battery chemistry that can surpass the performance of currently used lithium-ion batteries (LIBs) is of utmost importance for resolving global concerns related to the shortage of fossil fuels as well as global climate change. Electric vehicles and large-scale energy storage systems for renewable energies require higher performance than that offered by the current battery technology in terms of energy density, safety, and production cost. As the LIB technology cannot meet the requirements of those new applications, extensive research efforts have been devoted to search for alternative battery systems with a higher energy density combined with safer operation and cheaper production, namely, post-LIBs.[1–3] Li−O_2 and Li−S battery systems are typical examples, as they have some advantages over conventional LIB systems, including high energy density.[4] Recent intensive research efforts have achieved significant progress in the development of post-LIBs systems, rendering them to be likely power sources for the above-mentioned emerging applications.[5–7] The basic design of these battery systems, including the underlying reaction chemistry, however, had been already developed about 20 years ago; [8,9] in other words, they are not recently invented systems. The remarkable technological advances in Li−S and Li−O_2 batteries might be owed not only to extensive research efforts in this field, but also to the recent achievements in material science and nanotechnology. For example, nanostructured carbon materials, as well as other nanoporous inorganic materials, can significantly improve the performance of Li−O_2 and Li−S batteries.[5,6] In this respect, it is worth revisiting another secondary lithium battery systems already developed, but not commercialized yet.

We found that the rechargeable Li−SO_2 battery, of which the basic chemistry had been developed by Dey et al. 30 years ago,[10] has enormous potential as a post-LIB system. First, the electrolyte composed of SO_2 and lithium tetrachloroaluminate salt shows substantially higher ionic conductivity (close to 0.1 S cm^{-1} at room temperature) than conventional organic electrolytes,[11] suggesting that the power density and rate capability of the battery adopting the SO_2-based electrolyte may be considerably higher than those of the organic electrolyte based cells. Second, the SO_2 based inorganic electrolyte is non-flammable,[12] which can substantially improve the safety of such batteries. Third, the electrochemical performance of the Li−SO_2 battery is comparable to those of the Li−O_2 and Li−S based batteries. The working potential is about 3 V (vs. Li/Li^+), which is higher than that of Li−S (2.0 V) and Li−O_2 (2.7 V), and the voltage hysteresis between charge and discharge in Li−SO_2 is much lower than that observed in Li−O_2 battery systems.[4] Although the theoretical capacity of the SO_2 based catholyte (219 mAh g^{-1} and 372 mAh cm^{-3}, based on the mass and volume of $LiAlCl_4 \cdot 3SO_2$, respectively) is lower than that observed in the case of the Li−O_2 and Li−S batteries, we found that the theoretical energy density of the rechargeable Li−SO_2 battery system (651 Wh kg^{-1}) is 68% higher than that of the conventional LIBs (387 Wh kg^{-1}).[13]

As already mentioned, the recent achievements in material science and nanotechnology have greatly enhanced the electrochemical performance of post-LIBs. From these results, we expect that the performance of the Li−SO_2 battery can be also significantly improved, if recently discovered nanostructured materials are properly exploited in the system. The electrochemical performance of the SO_2-based catholyte, including the capacity and cycle performance, is highly dependent on the microstructure of the carbon cathode used in the Li−SO_2 battery (see a schematic

illustration of Li−SO_2 battery system in **Fig. 1a** and also find the brief introduction to the reaction chemistry of Li−SO_2 battery system in the Supplementary Information).[10] This suggests that recently developed nanostructured carbon materials—for example, ordered mesoporous carbon and graphene—can remarkably improve the electrochemical performances of the Li−SO_2 battery. Herein, we demonstrate that nanotechnology can significantly enhance the battery performance of rechargeable Li−SO_2 systems, thereby eventually showing their considerable potential to become an attractive candidate for post-LIB systems.

Experimental

Materials preparation

KB-600JD (Ketjenblack EC-600JD carbon black, Akzo Nobel, Japan), MSP-20 (amorphous activated carbon, Kansai Coke and Chemicals Co., Japan), CS (spherical activated carbon, Suntel Co., Korea), rGO (reduced graphene oxide, Graphit Kropfmühl AG, Germany) were used as received for the cathode of Li−SO_2 cells. OMC (ordered mesoporous carbon) was synthesized by following a nano-replication method described elsewhere.[14] A mesoporous silica SBA-15 with 2-d hexagonal (P6mm) mesostructure and sucrose were used as the hard template and carbon source, respectively.

$LiAlCl_4 \cdot 3SO_2$ electrolyte was prepared as follows: LiCl (>99.9%, Alfa Aesar) was vacuum-dried at 120 ºC for 24 h prior to use, while anhydrous $AlCl_3$, (99.999%, Alfa Aesar) was used without any purification. The electrolyte was prepared by blowing SO_2 gas (anhydrous, Fluka) through a mixture of LiCl and $AlCl_3$ in a glass/Teflon vessel. The molar ratio of LiCl to $AlCl_3$ was 1.1 to avoid the presence of free $AlCl_3$,

which is known to be corrosive against alkali metals. As soon as SO_2 gas was in contact with the mixture, it became liquid of transparent light ocher color. The SO_2 gas was blown until the desired SO_2 concentration was reached, as determined by weighing the electrolyte vessel. After the reaction was completed, the electrolyte vessel was transferred back into the Ar-filled glove box and placed in a glass bottle containing small pieces of Li metal to remove possible residue of $AlCl_3$ or H_2O.

Characterization

X-ray diffraction (XRD) patterns were obtained using an Empyrean diffractometer (PANalytical) equipped with monochromated Cu Kα radiation (λ = 1.54056 Å). A lab-made swagelok-type in situ XRD cell was composed of the cathode made of OMC and polytetrafluoroethylene (PTFE, 10%), Li metal-sheet anode, and glass fiber separator, equipped with a beryllium (Be) disk on the cathode side to act as a X-ray window, as well as a current collector. The morphology, microstructure, and composition of the carbon materials and the electrodes were examined using field-emission scanning electron microscope (FESEM, JEOL JSM-7000F). For ex situ SEM observations of the cycled cathode, the cathode was carefully disassembled from the cell and then rinsed with $SOCl_2$ in an Ar-filled glove box to remove residual electrolyte since the $SOCl_2$ is known to dissolve SO_2 and $LiAlCl_4$.[15] Cross sections of the carbon electrode were prepared using the JEOL SM-09010 cross-section polisher (CP). The Brunauer−Emmett−Teller (BET) surface area, pore volume, and pore-size distribution of the carbon materials were determined by a Tristar II 3020 (Micromeritics) physisorption system using N_2 as adsorbate at 77 K. Information on the internal structure of the carbon-composite electrodes was acquired by a mercury-intrusion porosimeter (Autopore 9500, Micrometrics Inc.).

Electrochemical measurement

The carbon cathodes were prepared by mixing a PTFE emulsion (60% in water, Sigma-Aldrich) with a selected carbon wherein the content of PTFE was 10 wt.%. The carbon was wet relevantly with isopropanol (Daejung Chemcials, Korea) before adding the PTFE emulsion and the paste was well mixed until it became gummy. The final paste was then spread on Ni-mesh current collector and roll-pressed. The pressed carbon electrode was dried in vacuum oven at 200 ^{o}C for 1 h. The loading level of carbon and binder was 3.0−4.0 mg cm^{-2}. A Li-metal foil was used for the anode and a glass microfiber filter of 190 μm thickness (GC50, Advantec) was used as separator. 2032-type coin cells consisting of the electrodes, separator, and $LiAlCl_4 \cdot 3SO_2$ electrolyte were assembled in an Ar-filled glove box for discharge/charge tests. The assembled cells were aged for 12 h at room temperature and then electrochemically tested using a TOSCAT battery measurement system under the following protocols: The first and second cycles were operated galvanostatically at 100 mA g^{-1} within the voltage window of 2.9−3.9 V. In the following cycles, the current was set at 0.5C and 0.2C for discharging and charging, respectively. For the rate capability test, the discharge rate was varied from 0.1C to 2C at the fixed charge rate at 0.2C.

Results and discussion

We first properly selected five types of nanostructured carbon materials: KB-600JD, MSP-20, OMC, rGO, and CS (their nanostructure and powder morphologies are shown in **Fig. 1c−g** and **Fig. S1**†), and compared their electrochemical behaviors as cathode materials for rechargeable Li−SO_2 batteries. **Fig. 1b** shows the initial voltage profiles of the Li−SO_2 cells using the aforementioned carbon materials. The different carbon cathodes used in the Li−SO_2 cells delivered a broad range of

discharge capacities between 200 and 1700 mAh g^{-1}, closely related to the microstructure of carbon material. In particular, some carbon cathodes such as KB-600JD, rGO, and OMC exhibited reversible capacities above 1000 mAh g^{-1}, which are higher than that reported by Duracell about 30 years ago.[10] The specific capacity corresponds to an areal capacity higher than 3.0 mAh cm^{-2}, which is comparable to the typical values of commercial LIBs (3–5 mAh cm^{-2}) and significantly higher than those of reported Li–O_2 batteries.[4–6] The maximum theoretical energy density of the Li−SO_2 cells corresponds to 689 Wh kg^{-1} based on weight of the catholyte and the estimated energy density based on the weight of discharge products is 651 Wh kg^{-1} (**Table S1**†), which therefore much higher than those of conventional LIBs. Another merit of a Li−SO_2 cell is its high operating voltage of 3.15 V, which is considerably higher than those of the Li−S (2.0 V) and Li−O_2 (2.7 V) batteries.[4] Notably, the voltage hysteresis of the Li−SO_2 cells (0.5 V) is smaller than that of the Li−O_2 batteries (~0.7 V) [16–19], suggesting that the cathode reaction in the Li−SO_2 system is more reversible and the energy efficiency is relatively higher compared with that of Li-O_2 batteries (85% for Li−SO_2 and 78% for Li−O_2 battery). **Fig. 2a** shows the cycle performances of Li−SO_2 cells with various carbon cathodes. Given that the lithium-metal anode is virtually identical for all cells, the capacity retention characteristics of the Li−SO_2 cells can be mainly attributed to the cycle performance of the carbon cathode. While the KB-600JD and rGO cathodes showed continuous capacity fading during the cycling, the OMC cathode exhibited excellent capacity retention over 150 cycles, which was never found in the other reports on the development of a Li−SO_2 battery. The rate capability of the Li−SO_2 cells shows a similar tendency to their cycle performance. As shown in **Fig. 2b**, the OMC cathode exhibited a highly stable and superior rate capability to KB-600JD. While the KB-600JD cathode showed a drastic

capacity drop with increasing the rate, the OMC cathode delivered more than 70% of the capacity at a rate of 0.1C even at a high rate of 2C (= 2000 mA g^{-1}).

As displayed in the schematic illustration on the reaction mechanism of a Li−SO_2 cell (**Fig. 1a**), the discharge capacity of a Li−SO_2 cell is highly dependent on the type of carbon material used. Given that the underlying reaction mechanism in a Li−SO_2 system is the redox reaction of sulfur species from +4 to +3, thereby producing solid phases of LiCl and $LiAlCl(SO_2)_3$ on the surface of the carbon cathode,[13] it is not surprising that carbon materials with higher specific area allow a higher discharge capacity. To elucidate the correlation of the discharge capacity with various carbon properties, we quantitatively determined the specific surface area, pore size, and pore volume of the above-listed five different carbon materials using N_2 sorption−desorption isotherms (**Fig. S2†**); the results are summarized along with the discharge capacity in **Table 1** and **Fig. 3**. Remarkably, we could not find any relationship between the surface area and the reversible capacity, as shown in **Fig. 3a**. Although CS and MSP-20 show a fairly high surface area of over 2000 m^2 g^{-1}, their capacities are significantly lower than those of other carbon materials showing a smaller surface area (KB-600JD, OMC, and rGO). For example, the rGO electrode, which has a small surface area as low as 14% of that of MSP-20, delivers about ten times higher discharge capacity than the MSP-20 electrode. Furthermore, OMC delivered a smaller reversible capacity than KB-600JD, even though they have almost the same surface area. These counter-intuitive results indicate that the specific surface area of the carbon material is not the primary parameter in determining the capacity of a Li−SO_2 cell. As in the case of the surface area, a similar discrepancy was found between the pore volume and discharge capacity (**Fig. 3b)**. For example, we found a

large difference in the discharge capacity of rGO and MSP-20, although their pore volumes are almost identical.

On the other hand, we found that there is a close relationship between the discharge capacity and the pore size of the carbon materials (**Fig. 3c**). As shown in the pore size distribution of carbon materials (Supplementary Fig. S2b), the carbon materials with a pore size in the range of 20−120 nm, such as KB-600JD, rGO, and OMC, show higher capacities than other carbon materials. These correlations reveal that a higher discharge capacity could be obtained when using carbon materials with macropores or larger mesopores, which might be more beneficial to increase the discharge capacity, as they are less susceptible to blockage by insulating discharge products, compared to microporous or smaller mesoporous carbon materials. Our understanding of the relationship between the carbon properties and electrochemical performance of the Li−SO_2 batteries seems to agree well with prior discussions by Chervin et al.[20] and Ding et al.[21] on a Li−O_2 battery system, in which a critical impact of the pore size on the electrochemical performance of the Li−O_2 batteries was suggested. They stated that an insoluble solid discharge product, Li_2O_2, is formed at the cathode, and it gradually blocks the electrolyte and oxygen pathways, limiting the reversible capacity, rate capability, and cycle life of the Li−O_2 batteries.[6]

To gain further insights into the electrochemical performance of the Li−SO_2 cells with respect to the type of nanostructured carbon materials, we observed the microstructural changes of some carbon cathodes during the discharge and charge processes using SEM. As shown in **Fig. 4a and b**, a large number of cubic crystals with a relatively large size of a few micrometers were found at the surface of the discharged electrode (compare with the corresponding as-prepared electrodes shown in **Fig. 4c and d**). The elemental mapping obtained using energy-dispersive X-ray

spectroscopy (**Fig. S3†**) confirmed that the well-crystallized discharge product was LiCl, as also previously reported by Foster et al..[11] Upon subsequent charging, the discharge product, LiCl, clearly disappeared (**Fig. 4e and f**). This reversible formation and disappearance of the discharge product LiCl was further confirmed by the in situ XRD analysis of the OMC cathode in a Li−SO_2 cell during cycling, as presented in **Fig. 4g**. Considering the relatively large size and insulating properties of the discharge product, the interparticulate macropores in the carbon electrode might be also essential for determining the electrochemical performance of the Li−SO_2 batteries.

To understand the role of the macropores in the carbon electrodes, we characterized the pore structure using the mercury porosimeter analysis, which is more relevant in investigating the interparticulate pore structure in powder-composite type electrodes, where the pore size could vary from submicron to a few tens of micrometer. **Fig. 5a and b** shows the pore-size distribution of the carbon electrodes and the plots between the obtained pore parameters and the discharge capacity, respectively. These results on the carbon electrodes clearly show that the discharge capacity of the carbon electrodes is strongly related to their total pore volume. Given that the size of LiCl precipitated as a discharge product increased up to a few microns (**Fig. 4a and b**), the presence of a larger pore size in the electrode is favorable, as it acts as a buffering space to accommodate the insulating discharge products and consistently maintain the mass transport of the catholyte inside the electrode because of a reduced pore blockage. From these results, we can conclude that the macroscale pore volume in the carbon electrode also plays an important role in determining the capacity of the cathode reaction in the Li−SO_2 cell.

Although more studies are required to fully understand the remarkable cycle and rate performance of the OMC cathode, the improvement can be explained by (i) the

peculiar nanostructure of the OMC material and (ii) its highly macroporous powder-composite electrode structure. The uniformly distributed mesopores within the OMC cathode enable the fast transport of SO_2-solvated lithium cations and tetrachloroaluminate anions, thus facilitating the redox reaction of the catholyte in the Li−SO_2 cell.[22] In addition, the nanoconfinement effect of the redox reaction within the mesopores of OMC might be also responsible for the enhanced electrochemical reversibility, as discussed in the case of the similar battery systems of Li(Na)−O_2 [23,24] and Li(Na)−S [25,26] employing OMC as cathode material. The highly macroporous electrode structure of the OMC cathode (**Fig. 5e**) in comparison to the KB-600JD cathode (**Fig. 5j**), can also contribute to the improved cell performance. Since the repeated accommodation and dissolution of LiCl occur in the carbon electrode during cycling, the involved volume changes of the carbon electrode can cause mechanical and electrical degradation, as found similar phenomena in alloy-type Li-storage materials, such as Si and Sn-based anodes.[27,28] **Fig. 5c and d** show the cross-sectional SEM images of OMC electrode before and after discharge. We found that the volume change of OMC electrode is about ~6%, which is considerably smaller than that of KB-600JD electrode (~75%, **Fig. 5h and i**). Moreover, the discharged OMC electrode (**Fig. 5f and Fig. S4**†) still contains some macropores while most of the pores in the KB-600JD electrode are blocked by discharge products (**Fig. 5k**). These results indicate that the OMC electrode can effectively accommodate large-sized LiCl discharge product and supply the conduction pathway for the electrolyte with less pore clogging, which eventually leads to the excellent cycling performance of the Li−SO_2 cell. However, excessively large pores in the carbon electrode may weaken its mechanical properties, in turn causing structural failure during the electrode preparation and leading to the loss of the electrical contact and fast capacity fading

during cycling.[21] The poor cycling performance of the rGO electrode can be explained by this hypothesis. The rGO electrode revealed significantly larger internal macro-channels (**Fig. S5**†) and delivered the highest initial discharge capacity of ~1190 mAh g^{-1}. However, in our study, the rGO electrode exhibited some structural instability during its preparation, finally leading to a poor cycling performance.

To further confirm the effect of the microstructure of the carbon electrode on the cycle performance of the Li−SO_2 cells, we observed the cycled OMC and KB-600JD electrodes after 100 cycles using SEM. The images reveal a large number of white solid precipitates, namely LiCl, on the KB-600JD electrode after 100 cycles; the precipitates remain on the electrode even after charging (**Fig. 5l**). This result suggests a possible accumulation of the residual discharge product during repeated cycling, thereby continuously passivating the carbon surface and blocking the pore structure of the electrode, which eventually cause the capacity fading of the Li−SO_2 cells during cycling. On the other hand, we could not detect a noticeable amount of LiCl precipitates in the OMC electrode even after 100 cycles (**Fig. 5g**). Moreover, much of the initial porous structure of the OMC electrode still persisted, which indicates that the well-balanced meso and macroporous structure of the OMC electrode is desirable for the electrochemical performance of the Li−SO_2 batteries. Together with intrinsic outstanding properties of Li−SO_2 battery including the use of non-flammable electrolyte even in direct contact with open flame (**Fig. S6**†) as well as the considerably high ionic conductivity close to 0.1 S cm^{-1} (**Fig. S7**†), the highly reversible Li−SO_2 battery system with the theoretical energy density of 651 Wh kg^{-1} enabled by nanotechnology is worthy of regarding as an another candidate for post LIBs.

Conclusions

We revisited the rechargeable Li−SO_2 battery system using various recently developed nanostructured carbonaceous materials. The electrochemical performance of the Li−SO_2 cell could be greatly improved, which makes it a promising candidate as a post-LIBs system. We confirmed that the discharge capacity and cycle performance of the Li−SO_2 cells are highly dependent on the microstructural properties of the carbon materials, as well as on the electrode structure; hierarchical meso and macroporous structures in the carbon material and electrode are desirable to further enhance the capacity and cycle performance of the Li−SO_2 batteries. Such results provide us not only with new research directions towards high-performance Li−SO_2 batteries, but also illustrate how nanotechnology leads to the substantial improvement of old-fashioned rechargeable batteries to be regarded as an alternative to the currently used LIBs.

Acknowledgements

This work was supported by the Energy Efficiency & Resources Core Technology Program of the Korea Institute of Energy Technology Evaluation and Planning (KETEP) granted financial resource from the Ministry of Trade, Industry & Energy, Republic of Korea (No. 20132020000260)

Supplementary Information

† Electronic supplementary information (ESI) available: The brief introduction of reaction chemistry of Li–SO_2 battery system; SEM, N_2 adsorption–desorption and Hg

porosimeter data of various carbon materials and the electrodes; conductivity and flammability-test of $LiAlCl_4 \cdot 3SO_2$ electrolyte; estimation of energy density of Li–SO_2 system. See DOI: xxx/xxxxxxx

Notes and references

1 M. Armand and J.-M. Tarascon, *Nature*, 2008, **451**, 652−657.
2 D. Larcher and J.-M. Tarascon, *Nat. Chem.*, 2015, **7**, 19−29.
3 N.-S. Choi, Z. Chen, S. A. Freunberger, X. Ji, Y.-K. Sun, K. Amine, G. Yushin, L. F. Nazar, J. Cho and P. G. Bruce, *Angew. Chem. Int. Ed.*, 2012, **51**, 9994−10024.
4 P. G. Bruce, S. A. Freunberger, L. J. Hardwick and J.-M. Tarascon, *Nat. Mater.*, 2012, **11**, 19−29.
5 A. Manthiram, Y. Fu, S.-H. Chung, C. Zu and Y.-S. Su, *Chem. Rev.*, 2014, **114**, 11751−11787.
6 A. C. Luntz and B. D. McCloskey, *Chem. Rev.*, 2014, **114**, 11721−11750.
7 J. Christensen, P. Albertus, R. S. Sanchez-Carrera, T. Lohmann, B. Kozinsky, R. Liedtke, J. Ahmed and A. Kojic, *J. Electrochem. Soc.*, 2012, **159**, R1−R30.
8 K. M. Abraham and Z. Jiang, *J. Electrochem. Soc.*, 1996, **143**, 1−5.
9 E. Peled, A. Gorenshtein, M. Segal and Y. Sternberg, *J. Power Sources*, 1989, **26**, 269−271.
10 A. N. Dey, H. C. Kuo, P. Piliero and M. Kallianidis, *J. Electrochem. Soc.*, 1988, **135**, 2115−2120.
11 D. L. Foster, H. C. Kuo, C. R. Schlaikjer and A. N. Dey, *J. Electrochem. Soc.*, 1988, **135**, 2682−2686.
12 R. Hartl, R. Neueder and H. J. Gores, *Acta Chim. Slov.*, 2009, **56**, 109−114.
13 I. R. Hill, B. G. Anderson, M. Goledzinowski and R. J. Dore, *J. Electrochem. Soc.*, 1995, **142**, 3267−3273.
14 H. I. Lee, J. H. Kim, D. J. You, J. E. Lee, J. M. Kim, W. S. Ahn, C. Pak, S. H. Joo, H. Chang and D. Seung, *Adv. Mater.*, 2008, **20**, 757−762.
15 S.-B. Lee, S.-I. Pyun and E.-J. Lee, *Electrochim. Acta*, 2001, **47**, 855−864.
16 K. Liao, X. Wang, Y. Sun, D. Tang, M. Han, P. He, X. Jiang, T. Zhang and H. Zhou, *Energy Environ. Sci.*, 2015, **8**, 1992−1997.
17 D. Kundu, R. Black, E. J. Berg and L. F. Nazar, *Energy Environ. Sci.*, 2015, **8**, 1292−1298.
18 H.-D. Lim, H. Song, J. Kim, H. Gwon, Y. Bae, K.-Y. Park, J. Hong, H. Kim, T. Kim, Y.-H. Kim, X. Lepro, R. Ovalle-Robles, R. H. Baughman and K. Kang, *Angew. Chem. Int. Ed.,* 2014, **53**, 3926−3931.
19 Y. Chen, S. A. Freunberger, Z. Peng, O. Fontaine and P. G. Bruce, *Nat. Chem*., 2013, **5**, 489−494.
20 C. N. Chervin, M. J. Wattendorf, J. W. Long, N. W. Kucko and D. R. Rolison, *J. Electrochem. Soc.*, 2013, **160**, A1510−A1516.

21 N. Ding, S. W. Chien, T. S. A. Hor, R. Lum, Y. Zong and Z. Liu, *J. Mater. Chem. A*, 2014, **2**, 12433−12441.
22 Z. Guo, D. Zhou, X. Dong, Z. Qiu, Y. Wang and Y. Xia, *Adv. Mater.*, 2013, **25**, 5668–5672.
23 W.-J. Kwak, Z. Chen, C. S. Yoon, J.-K. Lee, K. Amine and Y.-K. Sun, *Nano Energy*, 2015, **12**, 123−130.
24 J.-B. Park, J. Lee, C. S. Yoon and Y.-K. Sun, *ACS Appl. Mater. Interfaces*, 2013, **5**, 13426−13431.
25 Q. Zeng, D.-W. Wang, K.-H. Wu, Y. Li, F. C. d. Godoi and I. R. Gentle, *J. Mater. Chem. A*, 2014, **2**, 6439−6447.
26 J. T. Lee, Y. Zhao, S. Thieme, H. Kim, M. Oschatz, L. Borchardt, A. Magasinski, W.-I. Cho, S. Kaskel and G. Yushin, *Adv. Mater.*, 2013, **25**, 4573−4579.
27 C.-M. Park, J.-H. Kim, H. Kim and H.-J. Sohn, *Chem. Soc. Rev.*, 2010, **39**, 3115−3141.
28 G. Jeong, Y.-U. Kim, H. Kim, Y.-J. Kim and H.-J. Sohn, *Energy Environ. Sci.*, 2011, **4**, 1986−2002.

Table and Figure captions:

Figure 1. (a) A schematic illustration for discharge reaction mechanism in a Li−SO_2 battery system. During discharge, the oxidation state of sulfur in $LiAlCl_4 \cdot 3SO_2$ catholyte change from +4 to +3, producing unstable $SO_2^{\bullet -}$ radical anion. The reduced $SO_2^{\bullet -}$ immediately displace Cl^- from $AlCl_4^-$ anion, producing LiCl and $LiAlCl(SO_2)_3$ which precipitate at the cathode [13]. (b) The first cycle voltage profiles of various carbon cathodes at 0.1C in Li−SO_2 cells. (c−g) TEM images of various carbon materials used in this study: (c) KB-600JD, (d) OMC, (e) rGO, (f) CS and (g) MSP-20.

Figure 2. (a) Cycle performance of various carbon cathodes in Li−SO_2 cells. For the cycle tests, discharge current is 0.5C and charge current is 0.2C. (b) Rate capability of OMC and KB-600JD cathodes in Li−SO_2 cells. The insets display the corresponding capacity retention and Coulombic efficiency during cycling.

Figure 3. Correlation plots of (a) specific surface area (BET) vs. discharge capacity, (b) total pore volume vs. discharge capacity, and (c) pore size vs. discharge capacity for various carbon materials. The physical parameters were obtained by N_2 adsorption–desorption isotherm analysis. Number 1 corresponds to KB-600JD, 2 to rGO, 3 to OMC, 4 to CS, and 5 to MSP-20.

Figure 4. SEM images of the carbon cathodes in Li−SO_2 cells during the first cycle: (a) the discharged OMC, (b) the discharged KB-600JD, (c) the pristine OMC, (d) the pristine KB-600JD, (e) the charged OMC, and (f) the charged KB-600JD cathode. (g)

In situ XRD patterns of the OMC cathode in a Li−SO_2 cell during the first cycle. The referred LiCl corresponds to JCPDS #4-0664, indicated by arrows.

Figure 5. (a) Pore size distribution of various carbon electrodes measured by mercury intrusion porosimeter and (b) the correlation plot between total pore volume and discharge capacity. The cross-sectional SEM images of the pristine (c,e) OMC and (h,j) KB-600JD electrodes. The cross-sectional SEM images of the discharged (d,f) OMC and (i,k) KB-600JD electrodes after 2 cycles. The SEM images of the charged state of (g) OMC and (l) KB-600JD electrodes after 100 cycles.

Table 1. Surface area and pore characteristics of various carbon materials with their discharge capacities in Li−SO_2 cells.

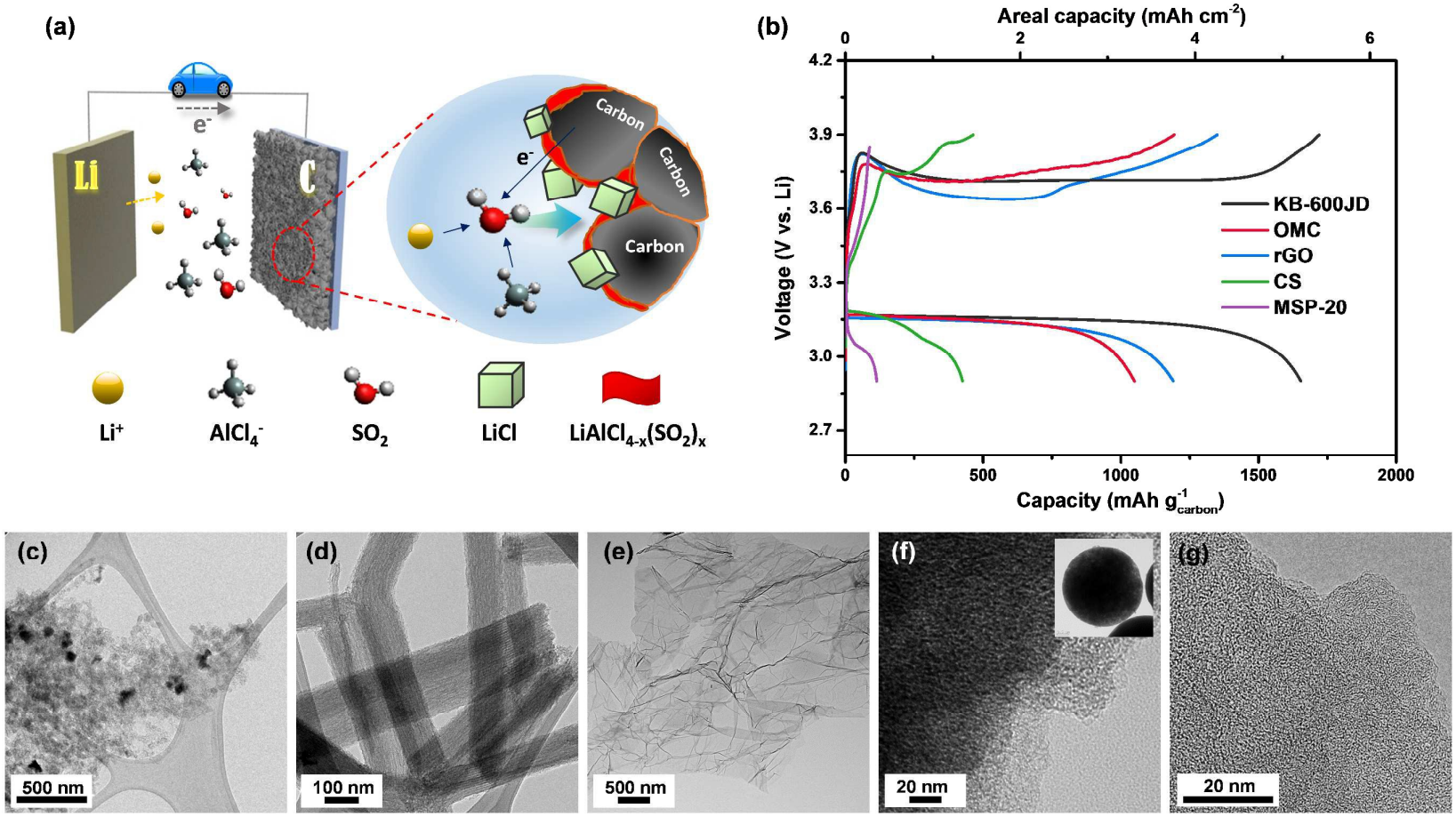

Figure 1

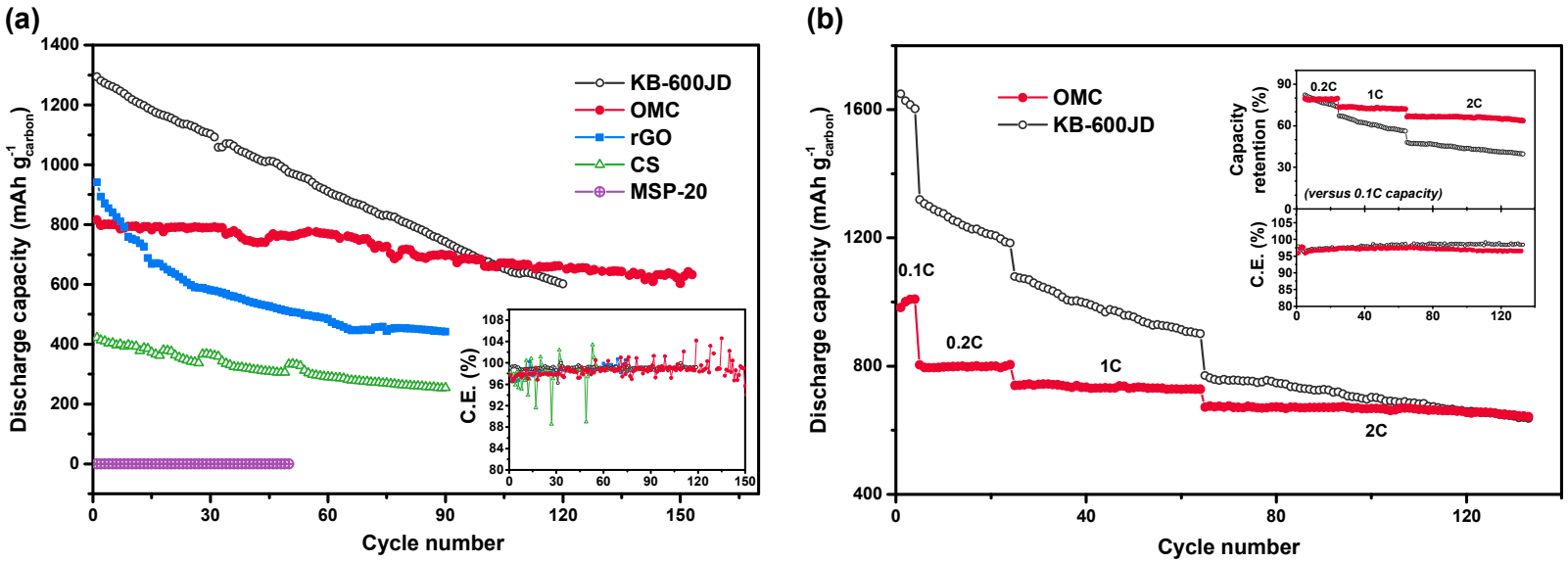

Figure 2

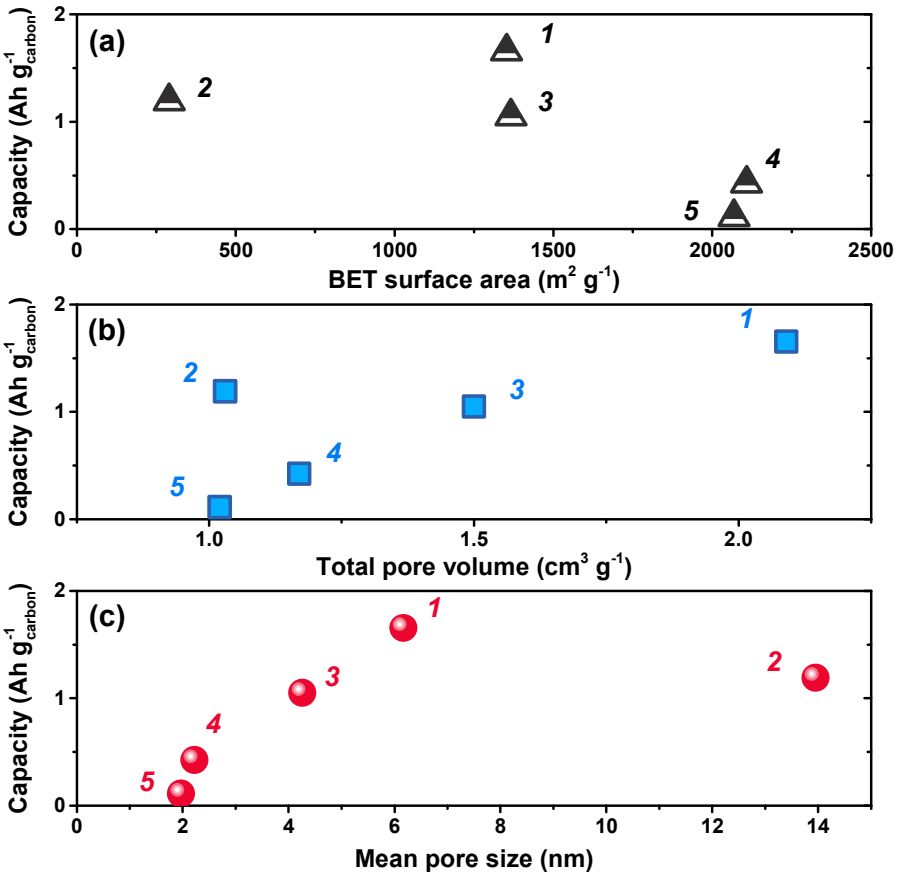

Figure 3

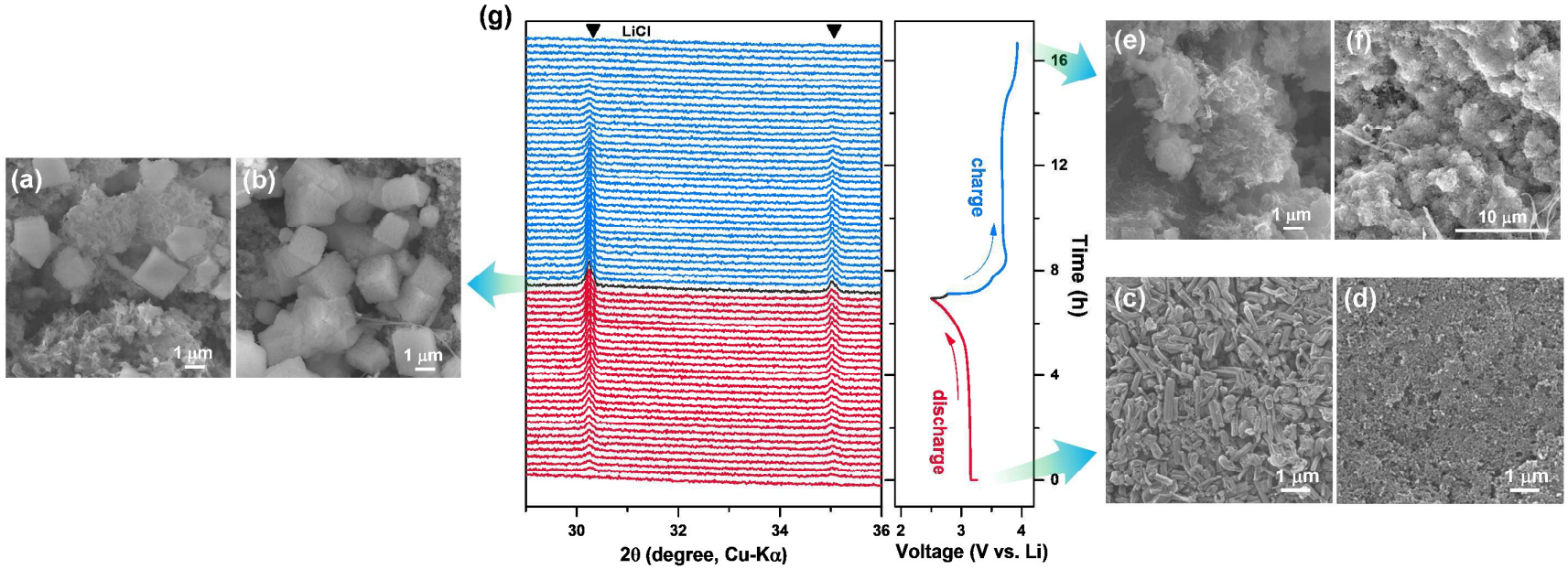

Figure 4

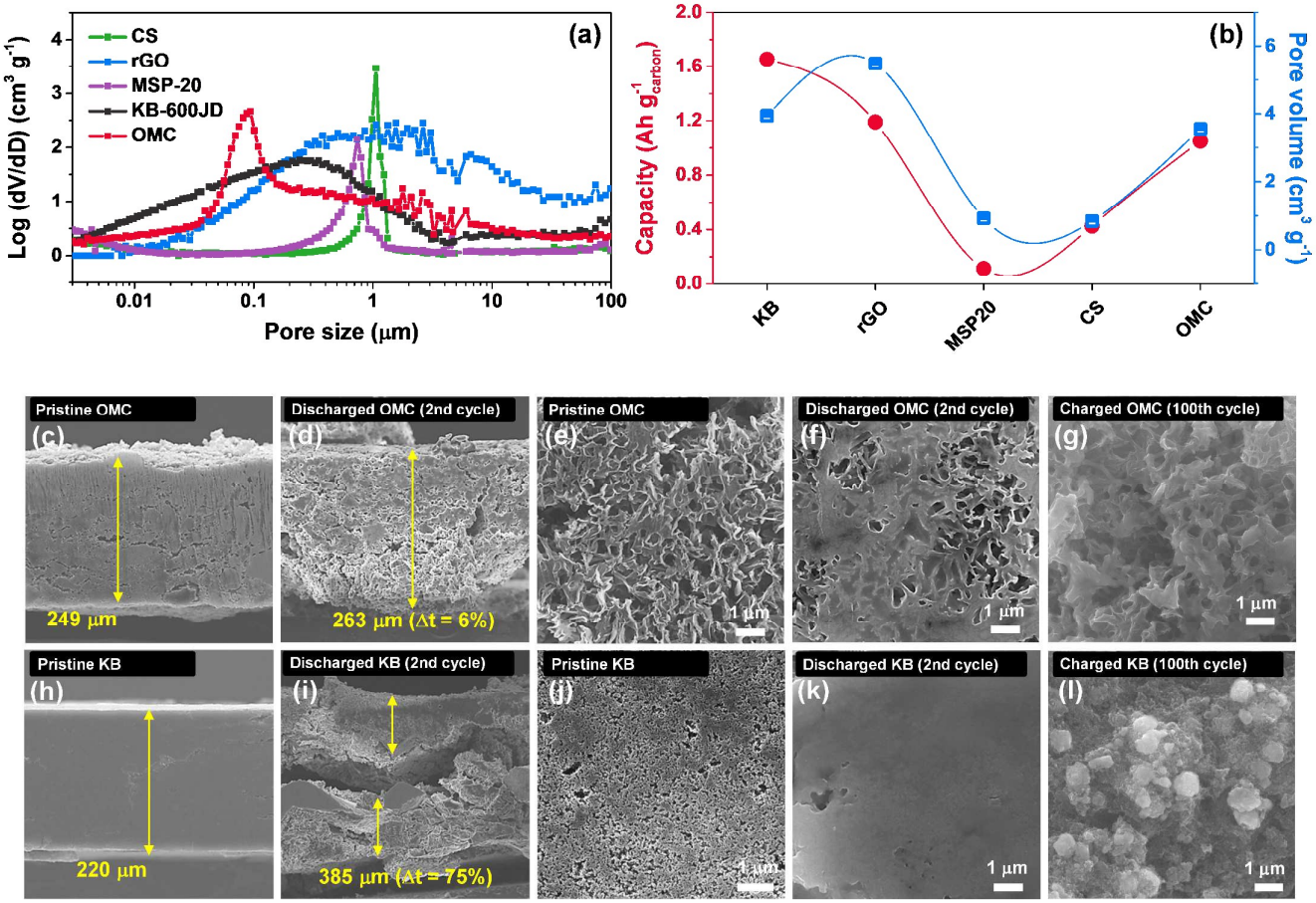

Figure 5

Table 1.

Carbon	BET surface area (m^2 g^{-1})	Pore size (nm)	Total pore volume (cm^3 g^{-1}) [a]	Micropore volume (cm^3 g^{-1}) [b]	Discharge capacity (mAh g^{-1})
KB	1353	6.17	2.09	0.06	1654
OMC	1367	4.26	1.5	0.068	1050
rGO	291	13.95	1.03	0.017	1190
CS	2108	2.22	1.17	0.093	425
MSP-20	2069	1.97	1.02	0.545	113

[a] Determined for pores between 1 and 120 nm from Barrett-Joyner-Halenda (BJH) using the adsorption isotherm.

[b] *t*-Plot micropore volume.

[*] All gram units in the table are for the carbon material in the cathode.

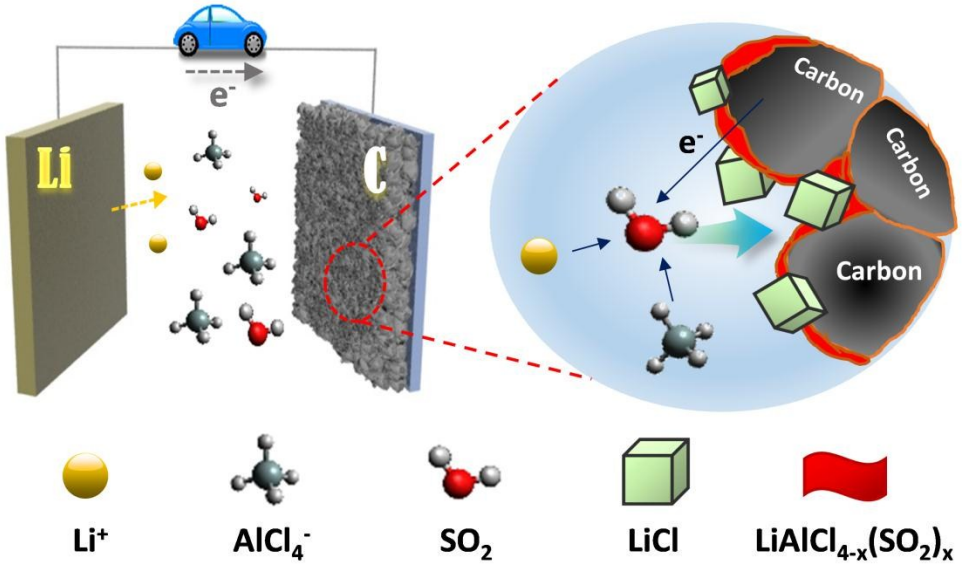

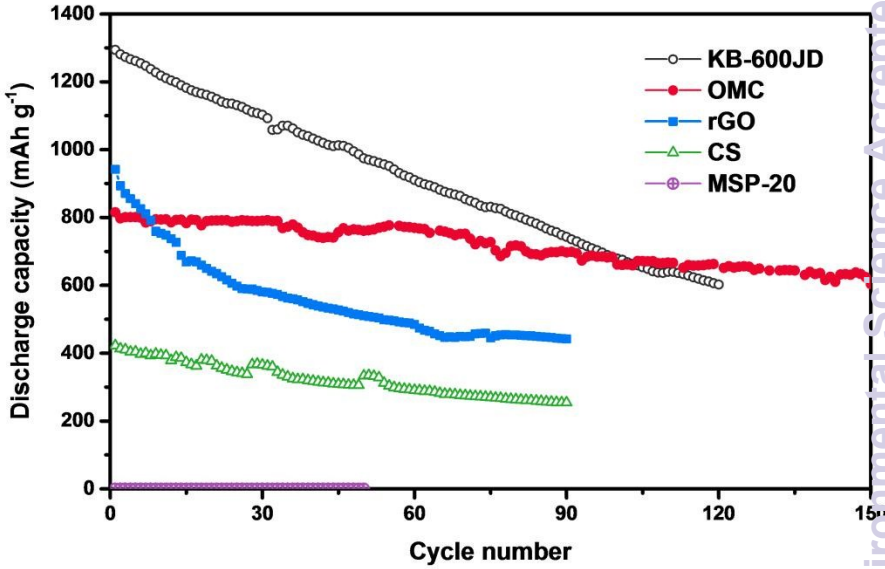

Broader context

New battery chemistry that can outperform currently used lithium ion battery in the energy density with comparable reliability is highly required to the requirement of emerging power source applications including electric vehicle and large-scale power storage system. Considering that recently progress of Li-S and Li-O_2 battery as a post lithium ion battery is possible by the wise use of nanotechnology, it is worthy of revisiting another lithium battery to show high energy density already developed, but not commercialized yet. Recent achievements in the nanotechnology can draw the full potential of Li-SO_2 rechargeable battery based on non-flammable SO_2 based inorganic electrolyte, thereby showing a reversible capacity of 1000 mAh g^{-1} with working potential of 3V and maintained the initial capacity up to 150 cycles without significant capacity fading. Such results provide us not only with new research directions towards high-performance Li−SO_2 batteries, but also clearly show how nanotechnology leads to the substantial improvement of old-fashioned rechargeable batteries to be regarded as an alternative to the currently used LIBs.